skin, and muscle biopsy did not confirm a respiratory chain defect in this child.

Patient #376 (F6, II:1, c.[98T>C];[176A>G], p.[Phe33-Ser];[Asn59Ser]), a girl, was born after an uneventful pregnancy at 39 weeks of gestation with normal birth measurements (weight 3124 g, length 51 cm) as the first child of unrelated Japanese parents. At the age of 2 days, she had epileptic seizures and was treated with phenobarbitone. In her first months, developmental delay and muscular hypotonia were noted. At the age of 8 months, she developed respiratory failure and unconsciousness, and was admitted to hospital. Transient lactic acidosis in blood (8.0 mmol/L, lower limit of normal 1.8 mmol/L) was found. Metabolic profiling (amino acid analysis, urine organic acid analysis, and acylcarnitine analysis) was unremarkable. Brain CT and MRI at 8 months showed symmetrical, bilateral signal abnormalities in basal ganglia, and she was diagnosed with Leigh-like syndrome. At the age of 1 year, she developed deafness, and at the age of 3 years dilated cardiomyopathy. Muscle biopsy showed mild deficiency of complex IV.

Patient #76656 (F7, II:2, c.[268G>A];[583G>A], p.[Gly90Arg];[Gly195Ser]), a girl, is the child of healthy unrelated German parents. After a normal pregnancy, she was born at term with normal birth measurements. The early motor development was normal, and she started walking at the age of 14 months. The girl was referred at age 2 years because of stiffness of gait and a tendency to fall. At admission, she showed muscular hypotonia, coordination problems, choreoathetotic movements, delayed speech development, and sensorineural deafness, which had been treated with hearing aids. Blood chemistry was normal including lactate, amino acids and organic acids.

Brain MRI at age 2 years showed no cerebral, cerebellar, or callosal atrophy but mild bilateral signal hyperintensities of putamen, globus pallidus, nucleus caudatus, and periventricular white matter. MR spectroscopy of basal ganglia showed mild elevation of lactate.

A muscle biopsy showed only unspecific morphologic findings, and biochemical analysis of respiratory chain activities was unremarkable.

Patient #MRB166 (F8, II:1, c.[161G>A];[394G>A], p.[Arg54His];[Ala132Thr]), a girl, is the first child of healthy unrelated German parents. Pregnancy was complicated by oligohydramnion and a diagnosis of gastroschisis. She was born by Cesarean section at 34 weeks of gestation with normal birth measurements (weight 1490 g [3rd percentile], length 41 cm [25th percentile], and head circumference 31 cm [25th percentile]). Surgical correction of gastroschisis was performed. The girl needed phototherapy for icterus neonatorum, tube feeding, and assisted ventilation. Deafness was diagnosed with 2 years of age and treated by cochlear implants. One seizure was observed at the age of 7 years. She showed truncal hypotonia, gait ataxia, and severe developmental delay (crawling at 1.5 years, sitting at 3 years, assisted walking at 5 years of age and no speech at 8 years). She has an oval face, a broad nasal tip, a large mouth, a high arched palate, and a receding chin. MLPA PWS/AS, *UBE3A*, and *MECP2* mutation analysis and microarray gave normal results.

Patient #57277 (F9, II:2, c.[161G>A];[431dup], p.[Arg54His];[Leu145Alafs*6]), a girl, is the second child of healthy nonconsanguineous parents from Germany. She was born after a normal pregnancy at 41 weeks of gestation with normal body measurements. Early motor development was delayed, and she never acquired the ability to sit or walk independently. Acquisition of language was impeded by sensorineural deafness for which she was fitted with hearing aids. At 18 months parents noted a pendular nystagmus with a rotatoric component as well as loss of central vision due to optic atrophy. Residual vision at 10 years was 0.3. From 2 years of age her motor abilities deteriorated during episodes of febrile illness and lactic acidemia when she developed a movement disorder that undulated between dystonia (opisthotonus) and chorea. Treatment with Levodopa/Carbidopa worsened her symptoms. She is presently 16 years old. Her body length is at and her weight 1 kg below the third percentile. Due to dysphagia and her inability to chew she has to be fed minced food. Massive caries and enamel defects from trismus required general dental repair and reconstruction under anesthesia. She visits a secondary school for disabled children, and communicates through a voice computer by saying "yes" or "no" or by making hand gestures.

Cranial MRI at the age of 1.5 years showed Leigh-like lesions with increased T2-signal intensity in the *putamen* and *globus pallidus* which became more prominent until age 2.2 years (Fig. 3C). Proton spectroscopy in the basal ganglia showed an increased lactate peak. Laboratory examinations revealed mildly increased urine excretion of lactate and lactic acidemia (2.5–4.0 mmol/L). The amino acid profile was normal in cerebrospinal fluid (CSF) and plasma. CPK was normal and muscle biopsy at 2 years of age only showed unspecific myopathic changes. Biochemical investigation revealed normal activities for the OXPHOS complexes, CS, PDHc as well as in vitro pyruvate oxidation.

Patient #52236 (F10, II:1, c.[229G>C];[476A>G], p.[Glu77Gln];[Gln159Arg]), a girl, is the first child of healthy unrelated German parents. After a normal pregnancy, she was born at 42 weeks of gestation with normal birth measurements (weight 3120 g, length 51 cm). Motor development was considered normal during the first months of life, and she started walking at the age of

11 months. From this age, however, short episodes of fist clenching, teeth gnashing, horizontal nystagmus and unresponsiveness were noted. Although repeated EEG did not show epileptic discharges, treatment with phenytoin was started and maintained until age 5 years when the attacks disappeared. From age 17 months, progressive gait abnormalities were observed. These were episodic in the beginning, but evolved into a paraspastic gait in early childhood, and the girl became wheelchair-dependent at age 9.5 years. From age 2 years, visual problems became evident, and examination showed bilateral optic atrophy. Visual acuity at age 13 years was 1/50 for both eyes. From age 7 years, progressive sensorineural deafness was found, and the patient was supplied with hearing aids at age 9.5 years. At the same age, mild mental retardation and dysarthria were noted. The patient completed a secondary school for blind children, and has been working in a workplace for disabled persons from age 18 years.

Examination at age 31 years showed short stature (155 cm) and low body weight (40 kg). Visual acuity was off-chart, the patient could only notice hand movements, and there was a pendular nystagmus of the blind. Communication was impeded by severe dysarthria. She had generalized dystonia and a spastic tetraparesis, leading to an inability to walk independently. Sensation was entirely normal.

Electromyography (EMG), neurography and repeated EEG were normal. Laboratory examinations showed mildly elevated lactate (2.5 mmol/L, normal <1.8 mmol/L) in CSF and inconsistently in serum (2.0–2.8 mmol/L, normal <2.2 mmol/L). A muscle biopsy at age 9 years showed some type II fiber atrophy due to immobilization and a faint accumulation of lipid droplets in single fibers. There were no ragged red fibers (RRF) and no cytochrome *c* oxidase (COX) deficiency, and biochemical analysis of respiratory chain activities showed normal results. Brain MRI at age 15 years showed exclusively Leigh-like signal hyperintensities in the *caput nuclei caudati* and *putamen* bilaterally (Fig. 3D). MR spectroscopy of the left *putamen* showed no elevation of lactate.

Genetic analysis

We used a dual approach of exome sequencing and panel sequencing to analyze a cohort of patients with suspected mitochondrial disorders. Seven index patients (#52236, #57277, #68552, #68761, #73663, #76656, and #MRB166) were investigated by exome sequencing in Germany as described previously.[8,9] In brief, we used a SureSelect Human All Exon 50 Mb Kit (Agilent) for enrichment and a HiSeq2500 (Illumina) for sequencing. Reads were aligned to the human reference assembly (hg19) with BWA (version 0.5.8 Open source software, Wellcome Trust Sanger Institute). More than 90% of the exome was covered at least 20× allowing for high-confidence variant calls. Single-nucleotide variants (SNVs) and small insertions and deletions were detected with SAMtools (version 0.1.7 Open source software, Wellcome Trust Sanger Institute). Variant prioritization was performed based on the autosomal-recessive patterns of inheritance and the notion that the clinical mitochondrial phenotype of the patients is very rare. We therefore excluded variants with a frequency higher than 0.1% in 3850 control exomes and public databases and focused on genes encoding mitochondrial proteins[10] carrying two potentially pathogenic DNA variants. In two other patients (#346 and #376) we used a TruSeq Exome kit from Illumina. A detailed description of the bioinformatic pipeline and variant filtering used for these two cases has been published recently.[11]

In patient #42031 we applied targeted enrichment of 1476 nuclear genes (including 1013 genes coding for mitochondrial proteins according to the MitoCarta) using an in-solution hybridization capture method (NimbleGen Madison, WI, USA). Paired-end sequencing was performed on a HiSeq2500 (Illumina) to an average 178× coverage. Sequence alignment and variant calling was done with CLC Workbench v.7.0.4. CLC bio, Aarhus, Denmark

We used Sanger sequencing to confirm all identified *ECHS1* mutations and to test the carrier status of available family members. Primer sequences and PCR conditions are available upon request.

Western blotting

Immunoblotting was performed using two different protocols. For the analysis of F2;II:1 (#42031), F10, II:2 (#52236), F9,II:2 (#57277), F5, II:3 (#73663) 45 μg of protein of patients' fibroblast cell homogenates were separated on 13% sodiumdodecyl sulfate polyacrylamide gel electrophoresis (SDS-PAGE) along with a protein standard (Precision Plus Protein Kaleidoscope, Biorad Hercules, CA, USA) and blotted onto polyvinylidine fluoride membranes (Immobilon, Merck Millipore Darmstadt, Germany). Primary antibodies were as follows: ECHS1 (66117, Proteintech Chicago, IL, USA), β-actin (ab13822, Abcam Cambridge, UK). Chemiluminescence detection was performed on an Odyssey Biomedical: Phoenix, AZ, USA infrared imaging system according to the manufacturer's instructions. For the analysis of F1, II:2 (#346), and F6, II:1 (#376) mitochondria were isolated by homogenization of cells in mitochondrial isolation buffer (20 mmol/L HEPES, 4-(2-hydroxyethyl)-1-piperazineethanesulfonic acid pH 7.4, 220 mmol/L mannitol, 70 mmol/L sucrose, 1 mmol/L Ethylenediaminetetraacetic acid) with

2 mg/mL Bovine serum albumin. Cell homogenates were centrifuged at 700*g* at 4°C for 5 min and postnuclear supernatant was collected. Mitochondria were pelleted by centrifugation at 10,000*g* at 4°C for 5 min and mitochondrial pellet was resuspended in mitochondrial isolation buffer for subsequent size-separation on 10% gels by SDS-PAGE, and transfer to a methanol-activated PVDF membrane. Immunoblotting was performed with primary antibodies from GeneTex (ECHS1) and Abcam (HSP60). Chemiluminescence detection was achieved with ECL Select (GE Healthcare, Little Chalfont, UK) and the membrane was viewed with the LAS4000 (GE Healthcare, Little Chalfont, UK), according to the manufacturer's instructions.

Analysis of 2-enoyl-CoA hydratase activity

2-enoyl-CoA hydratase (ECHS1) activity was measured spectrophotometrically in fibroblast cell lysates following the absorbance of the unsaturated substrate crotonyl-CoA over time (15 min) as described.[12,13] Briefly, trypsinized fibroblasts were resuspended in reduced Triton-X-100 (0.2%) and lysed by sonification. Lysates were centrifuged at 700*g* for 5 min to remove cellular debris and protein concentrations were determined in supernatants by the BCA method. The reaction mixture consisted of: 100 mmol/L potassium phosphate buffer (pH 8) for a final concentration of, 0.1 mg/mL BSA and 50 μL of cell homogenate for a total of 15 μg of protein. The reaction was started with 50 μL of 250 μmol/L crotonyl-CoA for a final concentration of 25 μmol/L. Samples were measured at 37°C in UV cuvettes at 263 nm in a Shimadzu spectrophotometer. Enzymatic activity was calculated using a molar extinction coefficient of 6700. Enzymatic activity was normalized to the mitochondrial marker enzyme CS as previously described.[14] All reactions were performed in at least three independent experiments in triplicates with similar findings.

Palmitate loading assay

Palmitate loading in human skin fibroblasts of ECHS1 patients, healthy volunteers as negative controls and fibroblasts of patients with short- and medium-chain acyl-CoA dehydrogenase (MCAD) deficiency as disease controls were performed as previously described.[15] In brief, cell cultures were maintained in Dulbecco's modified Eagle medium (Invitrogen, Darmstadt, Germany) supplemented with 2 mmol/L glutamine, 10% fetal calf serum, 1% penicillin/streptomycin, and Fungizone™ (all from Invitrogen) at 37°C and 5% CO_2 in a humidified atmosphere until confluency. Palmitate loading was performed in serum- and glutamine-free minimal essential medium (Invitrogen) containing palmitic acid (200 μmol/L; Sigma-Aldrich Taufkirchen, Germany), L-carnitine (400 μmol/L; Sigma), and bovine serum albumin (0.4%; fatty acid-free; Sigma). After the end of the 96 h-incubation period, 10 μL aliquots of the cell culture media were collected and mixed with isotope-labeled internal standard (Cambridge Isotope Laboratories, Tewksbury, MA 01876) in methanol. Twenty-five microliters of the butylated sample were used to analyze the acylcarnitine profile by tandem mass spectrometry. For each sample at least two independent measurements were performed. The acylcarnitine concentration was normalized to the protein content of the fibroblast sample and expressed as nmol/mg protein.

For the analysis of palmitate-dependent mitochondrial respiration, control and patient fibroblasts were seeded at a density of 20,000 cells/well in 80 μL of high glucose Dulbecco's modified media (Gibco:Life Technologies, Darmstadt, Germany) supplemented with 10% fetal bovine serum (Invitrogen), 1% penicillin-streptomycin (Invitrogen) and 200 μmol/L uridine (Sigma) in a XF 96-well cell culture microplate (Seahorse Bioscience, North Billerica, MA, USA) and incubated overnight at 37°C in 5% CO_2. Culture medium was replaced with 160 μL of serum- and glutamine-free minimal essential medium (Invitrogen) supplemented with L-carnitine (400 μmol/L; Sigma), and bovine serum albumin (0.4%; fatty acid-free; Sigma) and cells were incubated for 24 h at 37°C in 5% CO_2. Palmitate-BSA complex was prepared according to the manufacturer's protocol (Seahorse Bioscience). Oxygen consumption rate (OCR) was measured using a XF16 Extracellular Flux Analyzer 2 (Seahorse Biosciences). OCR was determined with no additions; after addition of BSA (30 μmol/L) or palmitate-BSA conjugate (180/30 μmol/L).

Results

Exome sequencing identifies *ECHS1* mutations

We applied whole exome sequencing in a cohort of 435 individuals with a suspected disorder of mitochondrial energy metabolism and identified six unrelated affected individuals carrying two heterozygous or homozygous rare variants (minor allele frequency [MAF] <0.1%) in *ECHS1* (Fig. 2). Applying the same variant selection criteria to our in-house exome datasets from 3850 patients referred with presumed nonmitochondrial phenotypes revealed rare recessive-type *ECHS1* variants in one additional index case, F8, II.1 (#MRB166, Fig. 2). This patient was investigated in the context of an intellectual disability study but the relevance of the *ECHS1* variants was hitherto unclear. Clinical follow-up and review of medical reports revealed, however, that the neurologic features of this patient

(deafness, seizures, hypotonia, ataxia, and developmental delay) are very well compatible with a mitochondrial disorder. In contrast, it remains unclear whether the dysmorphic signs in this patient are related to the ECHS1 deficiency as dysmorphism is rather uncommon in mitochondrial diseases and was not found in any of the other ECHS1-deficient patients. The enrichment of rare biallelic *ECHS1* variants in genomes of individuals with a suspected mitochondrial disorder ($n = 7$) compared to 3850 control genomes was genome-wide significant ($P < 1.1 \times 10^{-7}$, Fisher exact test). In addition, in several individuals, *ECHS1* was the only gene coding for proteins with a predicted or confirmed mitochondrial localization harboring two rare DNA variants. We gained further evidence for a disease association of *ECHS1* by exome sequencing of 180 Japanese individuals with suspected mitochondrial disorders which identified two additional *ECHS1*-mutant individuals, F1, II.2 (#346) and F6, II.1 (#376, Fig. 2). By panel sequencing in a further patient with a similar clinical presentation we identified two heterozygous *ECHS1* mutations in F2, II:1 (#42031, Fig. 2). The combined approaches of exome and candidate gene sequencing identified a total of 13 different disease alleles in ten index patients. Pedigrees of investigated families and localization of identified *ECHS1* mutations as well as the evolutionary conservation of affected amino acid residues are shown in Figure 2B. All *ECHS1* mutations were confirmed by Sanger sequencing in the index patients. Carrier testing of available parental samples confirmed a biallelic localization of the mutations. DNA from the parents was not available in families F4 and F6, however, in the latter a compound heterozygous state of the mutations was confirmed by haplotype phasing. The healthy siblings of families F10, F9, F3, and F7 were either wild-types or heterozygous carriers. For families F3, F5, and F1, family history was positive for the occurrence of similar clinical conditions but no DNA samples were available for molecular tests from individuals F1, II:1 and F3, II:3.

Of the 13 different *ECHS1* mutations identified in our cohort, only one, c.431dup, p.Leu145Alafs*6, predicts a premature truncation and loss of function of the protein (Table S1). All other detected mutations are missense variants, indicating that a complete loss of ECHS1 function may be embryonic lethal. With the exception of the c.268G>A, p.Gly90Arg variant, all are predicted to be disease-causing (MutationTaster2).[16] Although all variants are rare (MAF < 0.05%), three mutations were identified in more than one family (c.161G>A, p.Arg54His, $n = 3$; c.176A>G, p.Asn59Ser, $n = 2$; and c.476A>G, p.Gln159Arg, $n = 2$), in each case with different mutations on the other allele. In addition, the c.476A>G, p.Gln159Arg mutation was found in the homozygous state in a third, consanguineous family. However, there is no mutational hotspot and the identified mutations are distributed across all eight coding exons of *ECHS1* except for exons 1 and 7 (Fig. 2B).

Functional consequences of *ECHS1* mutations

Next, we analyzed the consequences of *ECHS1* mutations in fibroblast cell lines. In six cell lines, we investigated ECHS1 protein levels and in four of them we measured 2-enoyl-CoA hydratase activity. SDS-PAGE separation of mitochondrial fractions and total cell lysates followed by immunodetection with an antibody against ECHS1 revealed a severe decrease in ECHS1 steady-state levels in all patient-derived fibroblast cell lines. To test the functional impact of *ECHS1* mutations, we determined 2-enoyl-CoA hydratase activity in the fibroblasts cell lysates from individuals F2, II.1 (#42031), F10, II:2 (#52236), F9, II:2 (#57277), and F5, II:3 (#73663). The 2-enoyl-CoA hydratase activity was markedly reduced in patients' cell lines with residual activities varying between 14% and 50% of controls (Fig. 3B).

Palmitate loading in fibroblasts of three ECHS1 patients induced an acylcarnitine profile very similar to that of short-chain acyl-CoA dehydrogenase (SCAD) deficiency. The characteristic metabolite, butyrylcarnitine, increased to 170%, 199%, or 273% of the upper normal range of the controls. In another ECHS1-deficient patient, however, butyrylcarnitine was within the range of controls (48% of the upper normal range). In comparison, butyrylcarnitine increased to 388% of controls in patient fibroblasts with SCAD deficiency and 44% in MCAD deficiency. These results indicate that ECHS1 deficiency results in a mild functional disorder of short-chain fatty acid oxidation.

This notion is further supported by the observation of reduced palmitate-dependent respiration in patient-derived fibroblasts compared to controls (Fig. 4C). Noteworthy, in the three cell lines tested for both 2-enoyl-CoA hydratase activity and palmitate-dependent respiration, the severity of defects correlated. Together, these data provide evidence for the pathogenicity of eleven *ECHS1* alleles.

Organic acids in urine

In analogy, organic acid analysis by gas chromatography/mass spectrometry in urine of patient #73663 revealed slightly elevated concentrations of ethylmalonate, a key metabolite of SCAD deficiency. Functional deficiency of short-chain fatty acid oxidation was also shown by intermittently elevated plasma fatty acids (250–780 μmol/L; normal <300 μmol/L) with concomitantly low normal

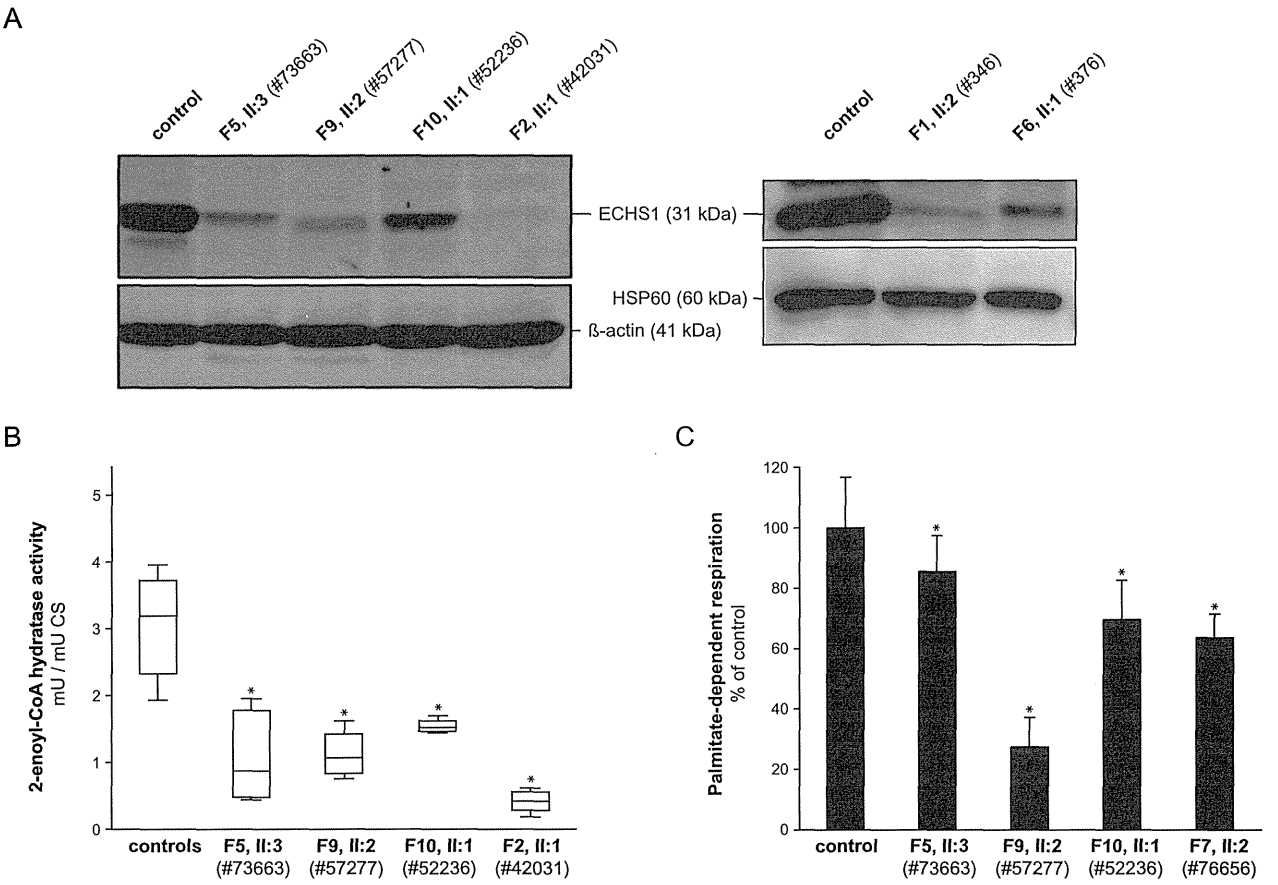

Figure 4. Analysis of ECHS1 levels and enzymatic activity. (A) Analysis of ECHS1 steady state levels by immunoblotting show a decrease in the amount of ECHS1 in patient-derived cell lines compared to controls. (B) Analysis of residual ECHS1 enzymatic activity indicates reduced 2-enoyl-CoA hydratase activity in cell lysates from patients' fibroblasts compared to controls. Results shown are from at least three experiments performed in triplicates and controls ($n = 4$). Boxplot whiskers indicate range from 5th to 95th percentile. *$P < 0.001$; two-tailed unpaired *t*-test. (C) Analysis of palmitate-dependent OCR in fibroblast cell lines revealed impaired respiration in patients' cells in comparison to controls. The experiment was performed several times with very similar results. The data are shown from one experiment performed with more than 10 replicates for each cell line grown and treated in parallel. Error bars indicate 1 SD. *$P < 0.001$; two-tailed unpaired *t*-test. ECHS1, short-chain enoyl-CoA hydratase; OCR, oxygen consumption rate.

plasma ketone bodies (65–90 μmol/L; normal <200 μmol/L) in postprandial state of some patients. However, ketogenesis was only mildly impaired which was shown by a mild increase in ketone bodies during catabolism (570–630 μmol/L, normal <3000 μmol/L). In addition, we identified 2-methyl-2,3-dihydroxybutyrate which likely derives from acryloyl-CoA or, alternatively, methacrylyl-CoA, both metabolites of valine oxidation, in urines of four ECHS1 patients. This metabolite correlated with disease severity as its concentration was 229-fold higher than the median value in 35 controls in the severely affected patient #42031 (onset at birth, died at 11 months), 39-fold higher in patient #73663 (onset on day 5, alive at 2 years), sixfold higher in patient #76656 (onset at 2 years, alive at 5 years), and even in the normal range in the mildest affected case #52236 (onset at 11 months, alive at 31 years), the only patient who survived into adulthood.

Phenotypic features of ECHS1 deficiency

In contrast to gene identification strategies in which an a priori phenotypic stratification of the investigated cohort was the main key to success,[17] this group of *ECHS1*-mutant individuals was identified by exome sequencing of a large cohort of individuals with suspected mitochondrial disorders. This approach allows for a rather unbiased assessment of the phenotypic spectrum associated with ECHS1 deficiency.

Disease severity ranged from presentations with neonatal onset and death in early infancy to survival into adulthood. In nine of 10 affected individuals, pregnancy was

normal and the children were born at term with normal body measurements. First clinical signs appeared in the prenatal period in one individual (oligohydramnios) and in the neonatal period (first month) in seven. Presenting signs included epileptic seizures, muscular hypotonia, respiratory and cardiac failure, failure to thrive, elevated lactate, and metabolic acidosis. In the two mildest affected individuals, developmental delay (F9, II:2, #57277) or episodic neurological symptoms (F10, II:1, #52236) were noted in the first year of life and lactate elevations were only intermittent and mild. While six of 10 affected individuals are still alive at the age of 2, 3, 5, 8, 16, and 31 years, four died at the age of 4, 11, 28, and 90 months, respectively. Interestingly, cardiomyopathy was only found in the individuals with a severe course and early death and none of the patients over 3 years of age.

In the course of the disease, neurological signs are most prominent including sensorineural deafness (9/9), developmental delay (8/10), epileptic seizures (6/9), dystonia (5/9), optic atrophy (6/10), muscular hypotonia (6/10), and spastic paresis (2/10). Other clinical features include cardiomyopathy (4/10) and respiratory failure (3/10). Increased blood, urine, and CSF lactate levels were found in seven of 10 individuals. Brain MRI was performed in nine of 10 individuals and showed white matter changes and brain atrophy in the very severe, early onset cases ($n = 5$) and Leigh-like bilateral T_2 hyperintensities in the basal ganglia (nucleus caudatus, putamen, and globus pallidus) in the less severely affected individuals ($n = 4$; Fig. 3). MR spectroscopy of basal ganglia showed elevated lactate concentrations in three of seven individuals.

Taken together, our findings identified *ECHS1* mutations as a cause of a new clinical entity characterized by an early onset, very severe (Leigh-like) mitochondrial encephalopathy with deafness, epilepsy, optic atrophy, and cardiomyopathy. Consistently elevated plasma concentrations of lactate indicate a dysfunction of the mitochondrial energy metabolism.

In view of the triad of (1) a severe progressive encephalopathy, (2) associated with bilateral basal ganglia lesions in MRI and autopsy, and (3) the mitochondrial dysfunction, ECHS1 deficiency is a new Leigh-like syndrome but can be differentiated from other forms of Leigh syndrome clinically and biochemically.

Analysis of OXPHOS enzymes in muscle tissue and fibroblasts

Since the clinical presentation suggested a mitochondrial disorder, eight of 10 patients received muscle and/or skin biopsies with detailed analysis of respiratory chain complexes, pyruvate dehydrogenase complex, ATP production, and pyruvate oxidation. Despite the severe clinical presentation of ECHS1 patients, only four of them showed mild and inconsistent changes in pyruvate oxidation (patient #42031), ATP production (patient #68761), and decreased activities of NADH:CoQ oxidoreductase (complex I of the respiratory chain) or cytochrome *c* oxidase (complex IV of the respiratory chain). Noteworthy, all these patients died (age of death: 4 months, 11 months, 3 years, 7.5 years), whereas four patients without documented changes in these analyses (#52236, #57277, #73663, #76656) have survived until now (age at latest visit: 2, 5, 16, and 31 years of life).

Discussion

ECHS1 is a mitochondrial matrix enzyme that is involved in several metabolic pathways including fatty acids and amino acids. Deficiency of this enzyme is expected to result in impaired mitochondrial fatty acid oxidation. However, as the membrane-bound enzymatic machinery of long-chain fatty acids remains intact, ketogenesis should not be completely disrupted in ECHS1-deficient individuals and, assumingly, the resulting clinical phenotype should be relatively benign – similar to SCAD deficiency.[18,19] In fact, ECHS1-deficient individuals showed mild to moderate hypoketosis, but did neither present with hypoketotic hypoglycemia and hypoglycemic encephalopathy nor were acylcarnitine profiles in blood suggestive of a mitochondrial β-oxidation disorder. Deficiency of short-chain fatty acid oxidation, however, was unmasked by palmitate loading of ECHS1-deficient fibroblasts (Fig. 4C). This metabolic challenge induced a selective increase in butyrylcarnitine in three of four patients tested, which in combination with slightly increased ethylmalonate in urine reflects impaired oxidation of short-chain fatty acids.

Despite this relatively mild metabolic derangement (concerning mitochondrial β-oxidation), ECHS1-deficient individuals presented with a severe clinical phenotype, with a high frequency of Leigh-like syndrome, neonatal lactic acidosis, sensorineural hearing loss, muscular hypotonia, cardiomyopathy, and respiratory failure. Although this combination of clinical findings, in particular the leading neurological presentation, is rather uncommon for fatty oxidation defects,[20,21] there is some clinical overlap with long-chain acyl-CoA dehydrogenase (LCHAD) deficiency and mitochondrial trifunctional protein (MTP) deficiency which resemble a primary OXPHOS deficiency. Affected individuals with LCHAD and MTP deficiency show a high frequency of neurological signs and symptoms including developmental delay, muscular hypotonia, epilepsy, and lipid storage myopathy as well as cardiomyopathy and sudden death in newborns and infants.[22,23] Similar to ECHS1 deficiency, elevated lactate is also often

found in LCHAD/MTP deficiency suggesting mitochondrial dysfunction.[22,23] In contrast to ECHS1 deficiency, however, individuals with LCHAD/MTP deficiency often present with hepatic dysfunction, retinopathy and peripheral neuropathy, but usually lack dystonia and sensorineural hearing loss. Interestingly, accumulating long-chain fatty acids and acyl-CoA are thought to act as mitochondrial toxins inhibiting energy metabolism in individuals with LCHAD and MTP deficiency.[24,25]

The striking discrepancy between an expected moderate impairment of mitochondrial fatty acid oxidation and the severe clinical presentation of ECHS1-deficient individuals argues for an additional pathomechanism. In addition to its function in fatty acid oxidation, ECHS1 has also been suggested to be involved in the L-isoleucine, L-valine and L-lysine oxidation using tiglyl-CoA, 2-methacrylyl-CoA or crotonyl-CoA, respectively, as a substrate (Fig. 1).[26] 2-Methacrylyl-CoA is a highly reactive compound and readily undergoes reactions with free sulfhydryl groups thereby inactivating important sulfhydryl-containing enzymes such as respiratory chain complexes and pyruvate dehydrogenase complex.[26] Accumulation of 2-methacrylyl-CoA has been considered as toxic compound in HIBCH deficiency, a disorder of the fifth step of valine oxidation with Leigh-like neurological phenotype and combined deficiency of multiple mitochondrial enzymes (Fig. 1).[4,5] The neurological phenotypes of individuals with ECHS1 deficiency and HIBCH deficiency are strikingly similar. As ECHS1 is suggested to catalyze the fourth step of valine oxidation, accumulation of 2-methacrylyl-CoA is expected and may be responsible for some of the pathological changes. Indeed, very recently, *ECHS1* mutations were reported in two siblings with Leigh disease and remarkable clinical and biochemical similarities to HIBCH deficiency,[6] with most prominent elevations of methacrylate and acrylate metabolites indicating deficiency of valine oxidation. Our observation of elevated levels of 2-methyl-2,3-dihydroxybutyrate in the urinary organic acids, a likely derivative of valine oxidation metabolites, provides further evidence for the involvement of defective valine metabolism in the pathogenesis of the disease. It may, in addition, be a useful biomarker of disease course as we observed some correlation already with the disease severity. Despite the clinical and biochemical similarities between ECHS1 and HIBCH deficiency, patients with ECHS1 deficiency showed less often impaired oxidative phosphorylation than those with HIBCH deficiency in the investigated fibroblasts or muscle biopsy samples. However, those ECHS1 patients with detectable OXPHOS deficiency had a severe course of disease and died during infancy or early childhood.

In conclusion, the identification of 10 unrelated individuals with *ECHS1* mutations allowed us to define the phenotypic spectrum of this new mitochondrial disease entity which can be differentiated clinically and biochemically from other molecular causes of Leigh or Leigh-like syndrome. Regarding pathogenesis, we found both a β-oxidation defect and impaired valine oxidation. We speculate that both defects contribute to the clinical and biochemical phenotype of this newly defined disorder. Intriguingly, ECHS1 deficiency may be amenable to treatment, provided that the elevation of toxic 2-enoyl-CoA compounds can be influenced by dietary intake. All possibly affected amino acids (valine, isoleucine, and lysine) in ECHS1 deficiency are essential amino acids and their dietary uptake can be expected to influence their catabolism. In addition, maintenance of high glucose levels, as recommended in fatty acid oxidation defects might be protective for the heart in ECHS1 deficiency. Anyway, further studies – preferably with an ECHS1 animal model – are necessary to unravel the exact pathomechanisms in ECHS1 deficiency and the efficacy and safety of possible treatments.

Acknowledgments

The authors thank K. Hirano, Y. Endo, T. Matsubayashi, and T. Nagatomo for referral of patient materials and T. Ottilinger for providing the autopsy images. This study was supported by the European Commission (FP7/2007-2013, under grant agreement number 262055 [ESGI], as a Transnational Access project of the European Sequencing and Genotyping Infrastructure); by the German Bundesministerium für Bildung und Forschung (BMBF) through the E-Rare project GENOMIT (01GM1207 for T. M. and H. P. and FWF I 920-B13 for J. A. M.), the German Network for mitochondrial disorders (mitoNET; 01GM1113A to B. B. and T. K., 01GM1113C to T. M., H. P. and P. F., and 01GM1113D to M. S.), the German Mental Retardation Network as part of the National Genome Research to T. M. S., D. W., and H. E. (grant numbers 01GS08164, 01GS08167, 01GS08163), and the Juniorverbund "mitOmics" (01ZX1405C); by the Deutsche Forschungsgemeinschaft (SFB 665 C4) to G. S. and M. S.; by a Wellcome Trust Strategic Award (096919/Z/11/Z) and UK NHS Specialized "Rare Mitochondrial Disorders of Adults and Children" Service to R. W. T., a Wellcome Trust WT098051 to R. D.; and by the Novartis Foundation for medical research and the Vinetum Foundation to A. S.; C. L. A. is the recipient of a National Institute of Health Research (NIHR) doctoral fellowship (NIHR-HCS-D12-03-04). This study was supported in part by a grant from the Research Program of Innovative Cell Biology by Innovative Technology (Cell Innovation), a Grant-in-Aid for the Development of New Technology from The Promotion and Mutual Aid Corporation for Private Schools of Japan from MEXT (to Y. O.), Grants-in-Aid for the

Research on Intractable Diseases (Mitochondrial Disease) from the Ministry of Health, Labour and Welfare (MHLW) of Japan to A. O. K. M. was supported by Kawano Masanori Memorial Public Interest Incorporated Foundation for Promotion of Pediatrics. The views expressed are those of the authors and not those of the funding organizations.

Author Contributions

Experiments were conceived by A. O., Y. O., J. N., S. K., T. M., and H. P. Patient phenotyping and review were performed by T. B. H., K. M., U. K., M. C. V., G. S., S. S., B. B., P. F., A. O., O. H., K. C., B. A., D. W., H. E., D. H., A. M. Z., R. W. T., R. J. R., R. T., W. S., G. F. H., M. S., S. K., and T. K. Sequence data generation, analysis, and interpretation were performed by T. B. H., A. S., T. W., E. G., A. O., Y. O., M. K., Y. K., Y. T., S. S., Y. M., A. K.-K., R. D., C. A., T. M. S., T. M., R. B., and H. P. Functional evaluation of mutations was performed and analyzed by C. B. J, L. S. K., E. G., S. E., and J. A. M. The manuscript was written by T. B. H., C. B. J., M. S., J. N., S. K., H. P., and T. K., and reviewed by all authors. T. B. H., J. N., S. K., H. P., and T. K. contributed equally.

Conflict of Interest

Dr. Cremer, Dr. Engels, Dr. Haack, Dr. Freisinger, Dr. Wieczorek, Dr. Zink, and Dr. Strom report grants from BMBF-German Bundesministerium für Bildung und Forschung during the conduct of the study. Dr. Ohtake reports grants from MHLW-Japanese Ministry of Health, Labour and Welfare, during the conduct of the study. Mrs Alston reports grants from NIHR-National Institute of Health Research during the conduct of the study. Dr. Taylor reports grants from UK Wellcome Trust, grants from UK NHS, during the conduct of the study. Dr. Durbin reports grants from European Commission, grants from UK Wellcome Trust, during the conduct of the study; other from Congenica Ltd, outside the submitted work. Dr. Eggimann reports grants from Stiftung Batzebär, outside the submitted work. Dr. Hoffmann reports grants from BMBF-German Bundesministerium für Bildung und Forschung and the Dietmar Hopp Foundation during the conduct of the study. Dr. Murayama reports grants from Kawano Masanori Memorial Public Interest Incorporated Foundation for Promotion of Pediatrics, during the conduct of the study; Dr. Büchner, Dr. Klopstock, and Dr. Prokisch report grants from European Commission and grants from BMBF-German Bundesministerium für Bildung und Forschung during the conduct of the study. Dr. Nuoffer reports grants from Stiftung Batzebär, from null, outside the submitted work; Dr. Okazaki reports grants from MEXT-Japanese Ministry of Education, Culture, Sports, Science and Technology, grants from MHLW-Japanese Ministry of Health, Labour and Welfare, during the conduct of the study; Dr. Schaller reports grants from Novartis Foundation, grants from Vinetum Foundation, during the conduct of the study; Dr. Schottmann reports grants from DFG-Deutsche Forschungsgemeinschaft, during the conduct of the study; Dr. Schuelke reports grants from BMBF-German Bundesministerium für Bildung und Forschung, grants from DFG-Deutsche Forschungsgemeinschaft, during the conduct of the study; Dr. Memari and Dr. Kolb-Kokocinski report grants from European Commission, grants from UK Wellcome Trust, during the conduct of the study. Dr. Meitinger reports grants from European Commission, grants from BMBF-German Bundesministerium für Bildung und Forschung, grants from DFG-Deutsche Forschungsgemeinschaft, during the conduct of the study. Dr Kölker reports grants from the European Union, DFG - Deutsche Forschungsgemeinschaft, Kindness-for-Kids Foundation, and Orphan Europe Sarl during the conduct of the study.

References

1. Kanazawa M, Ohtake A, Abe H, et al. Molecular cloning and sequence analysis of the cDNA for human mitochondrial short-chain enoyl-CoA hydratase. Enzyme Protein 1993;47:9–13.
2. Pougovkina O, te Brinke H, Ofman R, et al. Mitochondrial protein acetylation is driven by acetyl-CoA from fatty acid oxidation. Hum Mol Genet 2014;23:3513–3522.
3. Wanders RJ, Duran M, Loupatty FJ. Enzymology of the branched-chain amino acid oxidation disorders: the valine pathway. J Inherit Metab Dis 2012;35:5–12.
4. Ferdinandusse S, Waterham HR, Heales SJ, et al. HIBCH mutations can cause Leigh-like disease with combined deficiency of multiple mitochondrial respiratory chain enzymes and pyruvate dehydrogenase. Orphanet J Rare Dis 2013;8:188.
5. Loupatty FJ, Clayton PT, Ruiter JP, et al. Mutations in the gene encoding 3-hydroxyisobutyryl-CoA hydrolase results in progressive infantile neurodegeneration. Am J Hum Genet 2007;80:195–199.
6. Peters H, Buck N, Wanders R, et al. ECHS1 mutations in Leigh disease: a new inborn error of metabolism affecting valine metabolism. Brain 2014; The Netherlands.
7. Rahman S, Blok RB, Dahl HH, et al. Leigh syndrome: clinical features and biochemical and DNA abnormalities. Ann Neurol 1996;39:343–351.
8. Haack TB, Gorza M, Danhauser K, et al. Phenotypic spectrum of eleven patients and five novel MTFMT

mutations identified by exome sequencing and candidate gene screening. Mol Genet Metab 2014;111:342–352.
9. Haack TB, Haberberger B, Frisch EM, et al. Molecular diagnosis in mitochondrial complex I deficiency using exome sequencing. J Med Genet 2012;49:277–283.
10. Elstner M, Andreoli C, Ahting U, et al. MitoP2: an integrative tool for the analysis of the mitochondrial proteome. Mol Biotechnol 2008;40:306–315.
11. Ohtake A, Murayama K, Mori M, et al. Diagnosis and molecular basis of mitochondrial respiratory chain disorders: exome sequencing for disease gene identification. Biochim Biophys Acta 2014;1840:1355–1359.
12. Fong JC, Schulz H. Purification and properties of pig heart crotonase and the presence of short chain and long chain enoyl coenzyme A hydratases in pig and guinea pig tissues. J Biol Chem 1977;252:542–547.
13. Luis PB, Ruiter JP, Ofman R, et al. Valproic acid utilizes the isoleucine breakdown pathway for its complete beta-oxidation. Biochem Pharmacol 2011;82:1740–1746.
14. Jackson CB, Nuoffer JM, Hahn D, et al. Mutations in SDHD lead to autosomal recessive encephalomyopathy and isolated mitochondrial complex II deficiency. J Med Genet 2014;51:170–175.
15. Okun JG, Kölker S, Schulze A, et al. A method for quantitative acylcarnitine profiling in human skin fibroblasts using unlabelled palmitic acid: diagnosis of fatty acid oxidation disorders and differentiation between biochemical phenotypes of MCAD deficiency. Biochim Biophys Acta 2002;1584:91–98.
16. Schwarz JM, Cooper DN, Schuelke M, Seelow D. MutationTaster2: mutation prediction for the deep-sequencing age. Nat Methods 2014;11:361–362.
17. Haack TB, Hogarth P, Kruer MC, et al. Exome sequencing reveals de novo WDR45 mutations causing a phenotypically distinct, X-linked dominant form of NBIA. Am J Hum Genet 2012;91:1144–1149.
18. Gallant NM, Leydiker K, Tang H, et al. Biochemical, molecular, and clinical characteristics of children with short chain acyl-CoA dehydrogenase deficiency detected by newborn screening in California. Mol Genet Metab 2012;106:55–61.
19. van Maldegem BT, Duran M, Wanders RJ, et al. Clinical, biochemical, and genetic heterogeneity in short-chain acyl-coenzyme A dehydrogenase deficiency. JAMA 2006;296:943–952.
20. Saudubray JM, Martin D, de Lonlay P, et al. Recognition and management of fatty acid oxidation defects: a series of 107 patients. J Inherit Metab Dis 1999;22:488–502.
21. Tein I. Disorders of fatty acid oxidation. Handb Clin Neurol 2013;113:1675–1688.
22. den Boer ME, Dionisi-Vici C, Chakrapani A, et al. Mitochondrial trifunctional protein deficiency: a severe fatty acid oxidation disorder with cardiac and neurologic involvement. J Pediatr 2003;142:684–689.
23. den Boer ME, Wanders RJ, Morris AA, et al. Long-chain 3-hydroxyacyl-CoA dehydrogenase deficiency: clinical presentation and follow-up of 50 patients. Pediatrics 2002;109:99–104.
24. Tonin AM, Ferreira GC, Grings M, et al. Disturbance of mitochondrial energy homeostasis caused by the metabolites accumulating in LCHAD and MTP deficiencies in rat brain. Life Sci 2010;86:825–831.
25. Ventura FV, Ruiter J, Ijlst L, et al. Differential inhibitory effect of long-chain acyl-CoA esters on succinate and glutamate transport into rat liver mitochondria and its possible implications for long-chain fatty acid oxidation defects. Mol Genet Metab 2005;86:344–352.
26. Brown GK, Hunt SM, Scholem R, et al. beta-Hydroxyisobutyryl coenzyme A deacylase deficiency: a defect in valine metabolism associated with physical malformations. Pediatrics 1982;70:532–538.

Supporting Information

Additional Supporting Information may be found in the online version of this article:

Table S1. Annotation details on identified ECHS1 mutations.

DIAGNOSTIC PATHOLOGY

RESEARCH Open Access

Pathological similarities between low birth weight-related nephropathy and nephropathy associated with mitochondrial cytopathy

Toshiyuki Imasawa[1,2*], Masashi Tanaka[3], Naoki Maruyama[4], Takehiko Kawaguchi[1], Yutaka Yamaguchi[5], Rodrigue Rossignol[6], Hiroshi Kitamura[2] and Motonobu Nishimura[1,2]

Abstract

Background: Individuals born with a low birth weight (LBW) have a higher risk of developing kidney dysfunction during their lifetime and sometimes exhibit focal segmental glomerulosclerosis (FSGS) lesions in their glomeruli. We herein try to obtain other pathological characteristics of LBW-related nephropathy.

Methods: We retrospectively evaluated the renal pathology of four patients demonstrating FSGS with a history of LBW. Two mitochondrial cytopathy patients were also analyzed. DNA mutations were surveyed using a PCR-Luminex assay.

Results: In all four FSGS patients with a history of LBW, focal segmental glomerulosclerosis were detected. Interestingly, granular swollen epithelial cells (GSECs), which have previously been reported exclusively in patients with mitochondrial cytopathy, were also observed in the distal tubules and/or collecting ducts of all four patients with a history of low birth weight in this study. Electron microscopy revealed that these granular swollen epithelial cells included an increased number of enlarged mitochondria. Furthermore, cytochrome c oxidase subunit IV staining of patients with a history of low birth weight and patients with mitochondrial DNA mutations showed unbalanced expression patterns in glomeruli and a part of tubular cells. However, no mitochondrial gene mutations were detected in any of our four patients with low birth weight-related nephropathy.

Conclusions: This is the first report to show the pathological similarities not only in glomeruli but also tubuli between nephropathy with a LBW history and nephropathy with mitochondrial cytopathy.

Virtual Slides: The virtual slide(s) for this article can be found here: http://www.diagnosticpathology.diagnomx.eu/vs/13000_2014_181

Keywords: Focal segmental glomerulosclerosis, Low birth weight, Mitochondria, Granular swollen epithelial cell

Background

Low-birth-weight (LBW) is also associated with an increased risk of end-stage renal disease (ESRD) [1]. Studies of both humans and animals have shown LBW to be significantly associated with a decreased number of nephrons [2-4]. Brenner proposed the glomerular hyperfiltration theory in which adaptive mechanisms activated in response to nephron loss increases the capillary pressure and the incidence of glomerular hypertrophy [5,6]. This intraglomerular hypertension results in accelerated damage to nephrons with further nephron loss. This vicious cycle promotes the further progression of chronic kidney disease (CKD).

In particular, it is well known that representative glomerular changes in LBW individuals include focal segmental glomerulosclerosis (FSGS) [7]. Although intraglomerular hypertension is associated with the pathogenesis of FSGS, the clear mechanisms by which FSGS lesions are formed have not been clarified. Because detail pathological analysis sometimes gives a clue to assess the pathogenesis, we

* Correspondence: imasawa@cehpnet.com
[1]Kidney Center, National Hospital Organization Chiba-East Hospital, 673 Nitona-cho, Chuoh-ku, Chiba-city, Chiba 260-8712, Japan
[2]Clinical Research Center, National Hospital Organization Chiba-East Hospital, Chiba-city, Chiba, Japan
Full list of author information is available at the end of the article

herein evaluated LBW-related nephropathy (LBWN) in order to obtain more detail pathological characteristics.

Methods

Patients

From January 2006 to December 2011, we performed 472 kidney biopsies in our division. In these cases, there were four cases of FSGS among patients born with a birth weight under 2,500 g (according to the WHO definition of LBW). These four patients (LBW 1–4) were retrospectively evaluated pathologically and genetically. In addition, two patients (Mt 1 and 2) who were found to have mitochondrial DNA (mtDNA) mutations and underwent kidney biopsies to investigate the cause of their proteinuria were also evaluated. As normal controls for staining (N = 3), kidneys dissected because of kidney cancer were used.

Histological analysis

Briefly, kidney specimens fixed in 10% neutral buffer formalin followed by embedding in paraffin were used for a light microscopy analysis with routine staining, as follows: hematoxylin and eosin (HE), periodic acid-Schiff (PAS), Masson's trichrome stain and periodic acid-methenamine-silver (PAM)-HE stain. The kidney specimens used for the electron microscopy analysis were fixed in 2% glutaraldehyde (pH 7.3-7.4) followed by 2% osmium tetroxide (pH 7.3-7.4). For cytochrome c oxidase subunit IV (COX IV) staining, paraffin-embedded specimens were used. Following deparaffinization and antigen activation using 10 mM of boiled citrate buffer (pH 6.0), rabbit anti-COX-IV antibodies (clone 3E11) (Cell Signaling Technology, Inc., Danvers, MA) were used as the primary antibody. SignalStain® Boost IHC Detection Reagent (HRP, Rabbit) (Cell Signaling Technology, Inc.) was used to detect the rabbit primary antibody, according to the manufacturer's instructions.

Assay for detecting mitochondrial gene mutations

Blood samples (1 ml/each analysis) were collected in EDTA-2Na tubes. Following centrifugation, the pellets were used for the analysis. For the analysis of urine sediments, over 100 ml of urine was collected from each patient, and the pellets obtained after centrifugation were used for the analysis. Five slices (4 μm) of frozen kidney sections were used for the genetic analysis. A PCR-Luminex assay, which can be used to survey 61 different pathogenic mtDNA mutations, was performed according to our previously reported method [8].

Ethical considerations

This study was conducted in accordance with the "Ethical Guidelines for Clinical Studies" (Revised on December 28, 2004, Ministry of Health, Labour and Welfare of Japan). All medical professionals involved in this study were required to comply with these ethical standards. The local Ethics Committee of Chiba-East Hospital approved the study protocol (No. 22), and all subjects provided their informed consent to participate in this study.

Results

All four LBW-related nephropathy patients exhibited perihilar variants of FSGS in their glomeruli

The background characteristics of the patients are summarized in Table 1. All four LBWN patients underwent kidney biopsies in order to determine the etiology of their persistent proteinuria. All four LBWN patients were male, with a mean birth weight of 1,692 g. The gestational ages and the reasons for the low birth weight could not be fully assessed in these cases (The gestational age of LBW1 was 28 weeks and that of LBW2 was 38 weeks). No subjects had symptoms of myopathy or encephalopathy, a history of stroke-like episodes or difficulty hearing. Although all patients had no subjective symptoms, they were found to have proteinuria on periodic medical examinations. Only one (LBW 3) of the LBWN patients suffered from diabetes mellitus (with a five-year history). The kidney size tended to be smaller than normal, except in LBW 3 (Table 1). The light microscopy analysis revealed that the glomeruli of all LBWN patients exhibited FSGS (Figure 1). Patient Mt 1 was initially found to have proteinuria at 39 weeks of gestation and was subsequently referred to our hospital because the proteinuria persisted for one year after delivery. Although she had no symptoms of MELAS (mitochondrial myopathy, encephalopathy, lactic acidosis, stroke-like episodes), we found increased morphologically abnormal mitochondria in her podocytes (Figure 2A). Therefore, we evaluated her mtDNA at our hospital and detected an mtDNA mutation (3243 A > G). Patient Mt 2 was found to have proteinuria on a periodic medical checkup at 19 years of age. She also had no symptoms of MELAS. She refused an assessment of her serum lactate level. However, she had a brother with MELAS (3243 A > G), and a kidney biopsy revealed that her podocytes included increased mitochondria (data not shown). Her mtDNA mutation (3243 A > G) was diagnosed at another hospital. Although the characteristic glomerular change in patients with mitochondrial cytopathy is FSGS, as previously described in several reports [9-11], neither of our two patients with mtDNA mutations had apparent FSGS lesions in the evaluated glomeruli (data not shown). An electron microscopy analysis of the two patients with mtDNA mutations revealed that the glomerular epithelial cells contained an increased number of enlarged mitochondria and mild foot process effacement. On the other hand, we found no morphological abnormalities or increments in the number of mitochondria in any of the observed sections obtained from the LBWN patients (Figure 2B-D). However, the

Table 1 Summary of patients

Case	Age	Sex	BMI[1]	Birth weight (g)	BP[2] (mmHg)	eGFR[3] (ml/min/1.73m^2)	Urinary protein[4] (g/gCr)	Serum lactate[5] (mg/dl)	Long axis of kidney[6] (mm)	Number of total glomeruli	Global sclerosis[7] (%)	Segmental sclerosis[8] (%)	Glomerular hypertrophy[9]	Foot process effacement	mtDNA mutation[10]
LBW1	21	M	22.0	978	120/65	98	0.34	15.2	880	24	8.3	16.7	+	+	none
LBW2	20	M	21.0	1900	126/82	46	0.56	n.d.	848	4	0	25	+	+	none
LBW3	36	M	31.2	1400	125/75	74	1.35	n.d.	1208	14	42.9	7.1	+	+	none
LBW4	41	M	24.5	2465	121/70	63	0.83	15.8	988	20	15	10	+	+	none
Mt1	34	F	17.6	2720	115/63	48	0.29	9.1	936	11	45.5	0	-	+	3243 A>G
Mt2	28	F	17.5	3630	96/63	118	1.39	n.d.	953	16	0	0	-	+	3243 A>G

[1]BMI, body max index at the time of kidney biopsy.
[2]BP, blood pressure: BP at the time of kidney biopsy is expressed as systolic/diastolic.
[3]eGFR, estimated glomerular filtration: eGFR is calculated by Japanese GFR equation [12] from serum creatinine value, age, and sex at the kidney biopsy.
[4]The data of urinary protein is based on a urinalysis on the day of the kidney biopsy.
[5]Serum lactate is measured by an enzymatic assay (normal range: 3-17mg/dl). We did not measure the lactate values in three of six patients (expressed as "n.d.").
[6]The long axis of the left kidney was measured by an echogram just before the kidney biopsy.
[7]The rate of the number of globally sclerosed glomeruli/total glomeruli in the observed section is expressed.
[8] The rate of the number of segmentally sclerosed glomeruli/remnant glomeruli (total glomerular number minus GS glomeruli) is expressed.
[9]The existence of glomerular hypertrophy is defined when the diameter of capillary area is over 250μm [13].
[10]mtDNA mutation was surveyed in blood, urine, and kidney specimens by the PCR-Luminex method [11] except Mit2 patient, who was already diagnosed by a gene analysis in the other hospital.

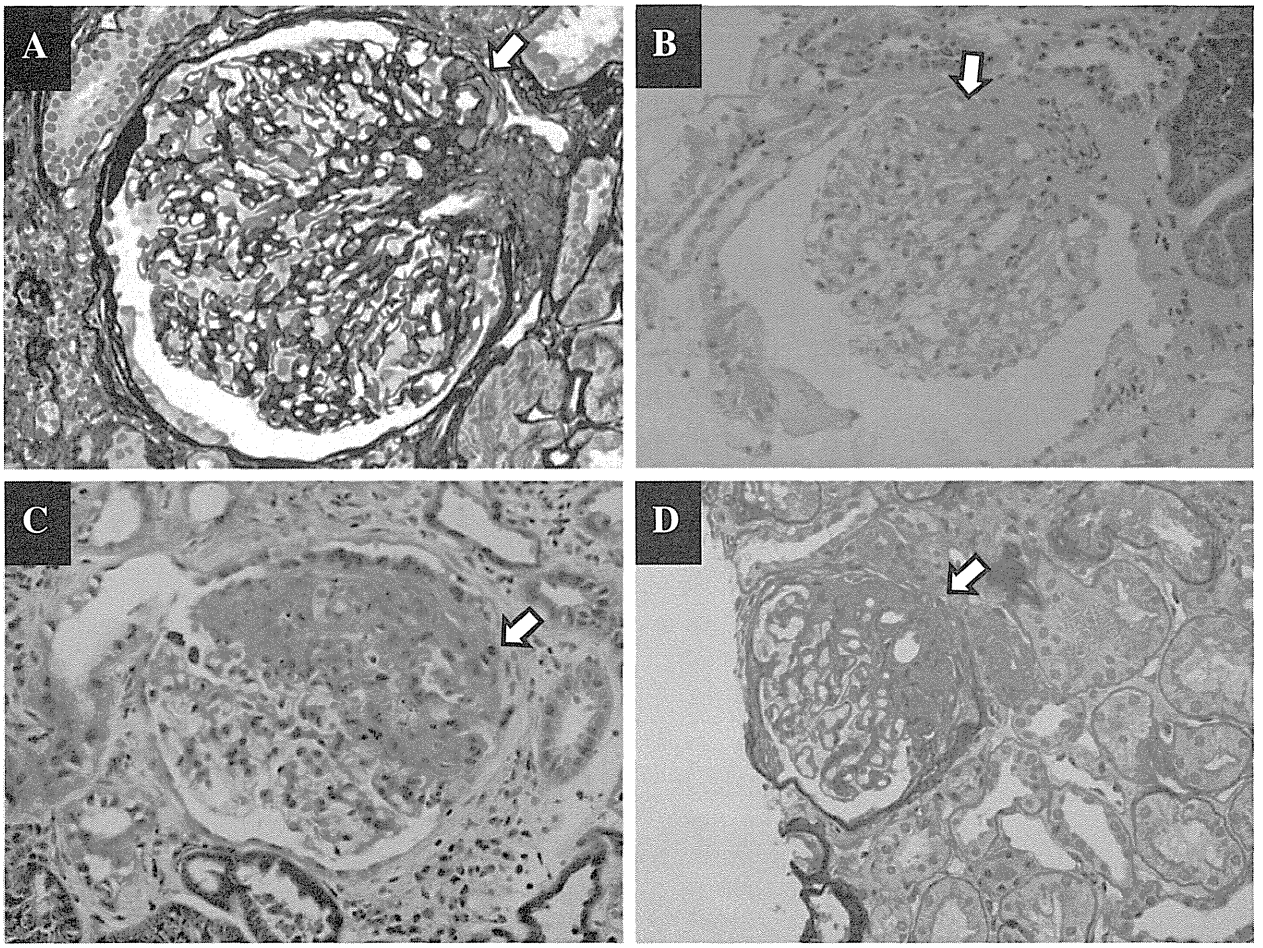

Figure 1 Representative photos of glomeruli in the FSGS patients born with LBW. (A): Exudative and sclerotic lesions are indicated in the perihilar area by arrows (LBW 1, PAM-HE stain). **(B)**: Segmental sclerosis in the perihilar area is indicated by the arrow (LBW 2, Masson's Trichrome stain). **(C)**: Segmental sclerosis is indicated by the arrow (LBW 3, Masson's Trichrome stain). **(D)**: Segmental sclerosis in the perihilar area is indicated by the arrow (LBW 4, PAS stain).

podocytes of the four LBWN patients showed mild foot process effacement (Figure 2B-D), similar to that observed in the patients with mtDNA mutations (Figure 2A).

All four patients with LBW-related nephropathy and the two patients with mtDNA mutations had granular swollen epithelial cells in their collecting ducts or distal tubules

The presence of granular swollen epithelial cells (GSECs) in the collecting ducts or distal tubules was recently reported to be a characteristic pathological change in patients with mitochondria cytopathy [14]. All four patients with LBWN as well as the two patients with mtDNA mutations had GSECs in their collecting ducts and/or distal tubules (Figure 3A-F). In addition, a portion of these GSECs had dropped out of the arrangement of the tubules. The electron microscopy analysis revealed that these GSECs contained an increased number of enlarged mitochondria (Figure 3G, H), and the nuclei occasionally seemed to be condensed.

The expression of Complex IV exhibited a mosaic pattern of staining in the glomeruli and tubules of both the LBW-related nephropathy patients and mtDNA mutation patients

Complex IV, which is composed of 13 subunits, is the terminal of the electron transfer chain in mitochondria. It was reported that the complex IV activity of podocytes changes in pathological conditions [15]. Therefore, we here stained for COX IV, which is one of the subunits. A COX IV expression analysis of normal controls showed that podocytes should be almost equally positive in the glomerulus (Figure 4A) and that tubular cells are also equally positive at the same luminal level (Figure 4B). However, in the LBWN patients, the expression of COX IV in the podocytes was unbalanced. Only a few podocytes appeared to intensely express COX IV, although the others expressed less COX IV (Figure 4C, E). In addition, the COX IV staining in a part of tubules of the LBWN patients exhibited a mosaic pattern, even at the same luminal level

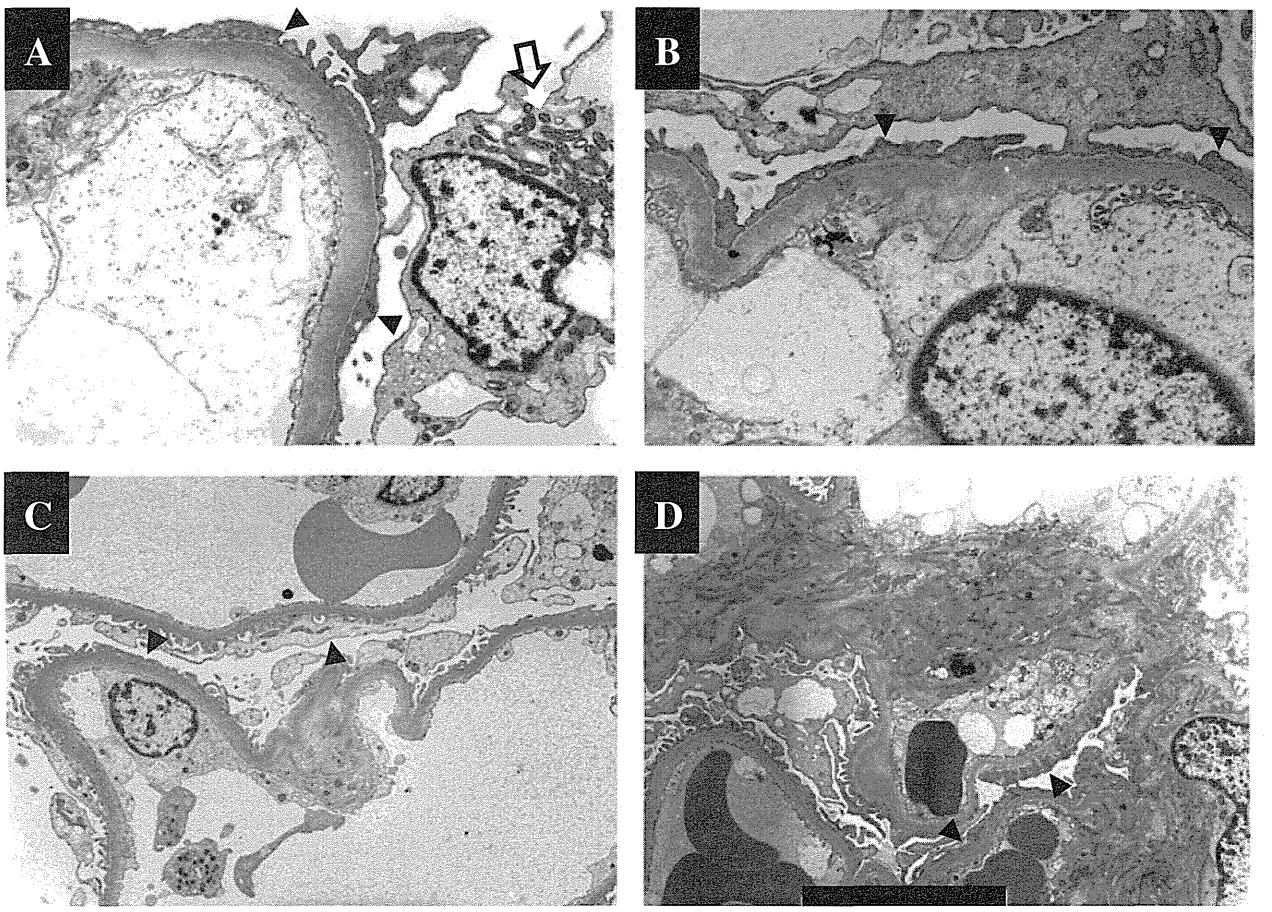

Figure 2 Electron microscopy of the glomeruli. (A): In Mt 1, a glomerular podocyte (indicated by the arrow) exhibits an increased number of mitochondria. The podocytes show patchy foot process effacement (arrowheads). **(B-D)**: In LBW 1 **(B)**, LBW 2 **(C)**, and LBW 3 **(D)**, the number and morphology of mitochondria in the glomerular podocytes are normal. However, the podocytes show patchy foot process effacement (arrowheads).

(Figure 4D,F). The cells strongly expressing COX IV appeared to correspond to GSECs. The expression patterns both of the glomerular podocytes and tubules in the patients with mtDNA mutations showed a mosaic pattern (Figure 4G, H), similar to that observed in the LBWN patients. The degree of the mosaic patterns in glomeruli and tubular cells should be more intense in patients with mtDNA mutations compared with LBWN patients.

The LBW-related nephropathy patients did not have any mitochondrial gene mutations

According to the PCR-Luminex assay, none of the 61 mtDNA mutations were detected in the blood, urine or kidney sections of the four LBWN patients (Table 1). However, an mtDNA mutation (3243 A > G) was clearly detected in all samples of blood, urine sediment and kidney sections in patient Mit 1. Because another patient (Mit 2) had already been found to have 3243 A > G mtDNA at another hospital, we did not perform an mtDNA mutation analysis using RCR-Luminex due to ethical considerations.

Discussion

Table 2 presents a summary of our results. The characteristic feature of glomerular involvement observed in patients with mitochondrial cytopathy is focal segmental glomerulosclerosis (FSGS), as previously described in a considerable number of reports [9-11]. In addition, it was recently reported that the presence of granular swollen epithelial cells (GSECs), in which enlarged mitochondria increase, in the distal tubules or collecting ducts is a specific pathological change in patients with mitochondrial cytopathy [14]. On the other hand, adults born with LBW have a high risk of kidney damage [1,16] and sometimes exhibit FSGS lesions in their glomeruli [7]. In this report, we showed that the pathological findings of kidney biopsy specimens were similar between patients with mtDNA mutations and those with LBWN with respect to the following three points (Table 2): 1. glomerular changes involve the presence of FSGS lesions and podocytes with foot process effacement; 2. a portion of tubular cells display characteristics of GSECs, in which the number of enlarged mitochondria is increased; and 3. The complex IV

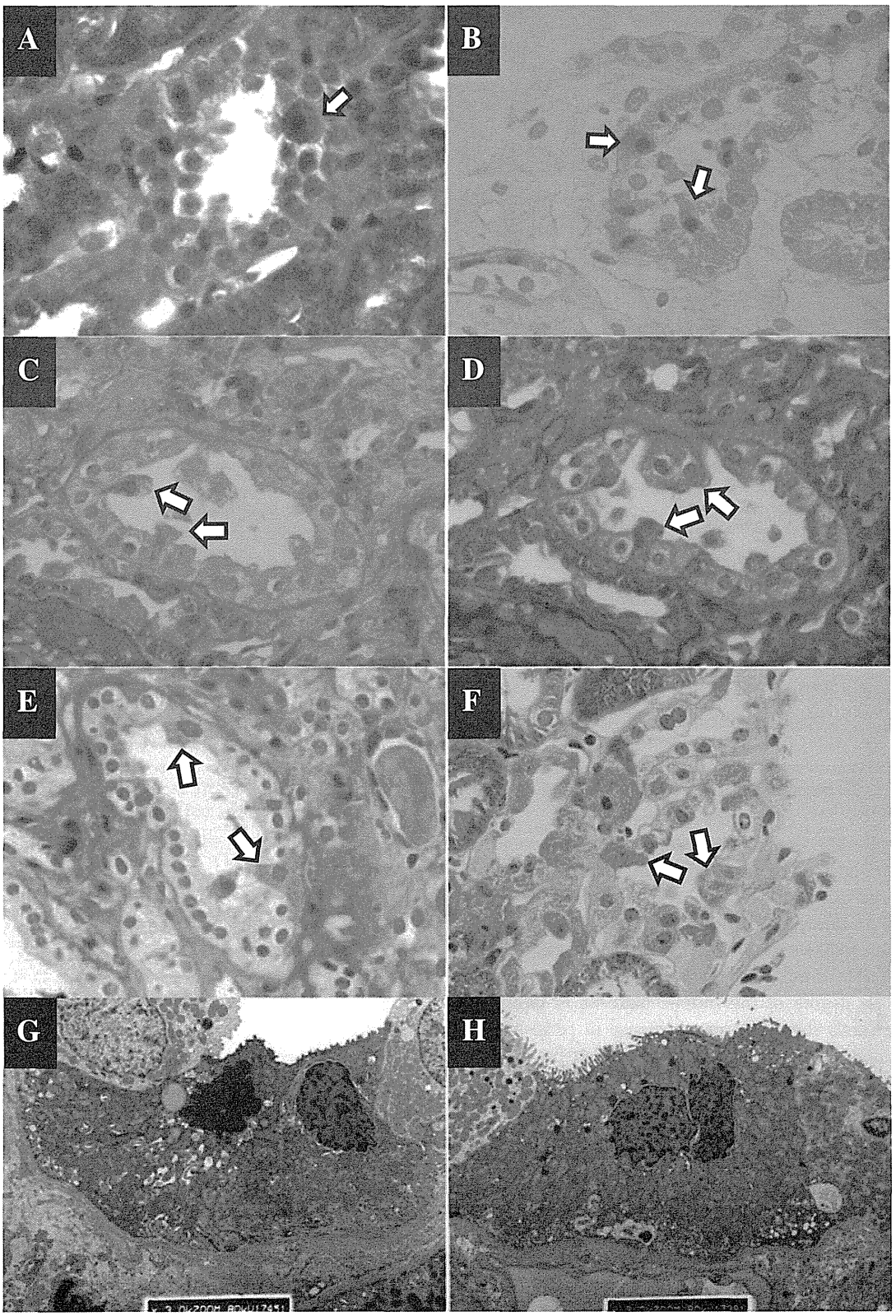

Figure 3 (See legend on next page.)

(See figure on previous page.)
Figure 3 Photos of tubules in patients of LBW-related nephropathy and patients with mtDNA mutation; (A)-(F): Masson's Trichrome stain, (G) and (H): electron microscopy (original magnification: × 3000). GESCs are present in collecting ducts or distal tubules of LBW 1 **(A)**, LBW 2 **(B)**, LBW 3 **(C)**, LBW 4 **(D)**, Mt 1 **(E)**, and Mt 2 **(F)**. In LBW 4 **(G)**, the number of mitochondria with morphological abnormalities is increased in the collecting duct. One nucleus appears to be condensed. In Mt 2 **(H)**, increased mitochondria are also observed in the cytoplasm of collecting duct.

expression shows an unbalanced expression pattern in a portion of podocytes and tubular cells. In fact, although our two patients with mtDNA mutations had no FSGS lesions, there is a possibility of sampling error. As another possibility, because these two patients had no other symptoms of mitochondrial cytopathy, the glomerular lesions could be slight. Furthermore, although we evaluated 5 obesity-related nephropathy with FSGS lesions (all patients are under 40-year-old), there were no GSECs.

Because the presence of GSECs in the tubules was previously described to be an exclusive characteristic change in patients with mitochondrial cytopathy (12), we initially suspected that the four patients with LBWN had certain mtDNA mutations. However, based on the PCR-Luminex method [8], which can be used to detect 61 different pathogenic mtDNA mutations, no mtDNA mutations were detected in the blood, urine sediment or kidney sections of the four patients with LBWN. Although these 61 mtDNA mutations include most mtDNA mutations previously reported in Japan [8], we cannot completely deny the existence of other mtDNA mutations in the four LBWN patients. The sensitivity of this method for surveying mtDNA mutations has previously been documented [8]. In addition, this method of detecting mtDNA mutations using blood, urine sediment and kidney sections was able to clearly detect the 3243 A > G mtDNA mutation in patient Mt 1. This report also provides a new strategy for detecting mtDNA mutations in nephropathy patients carrying mtDNA mutations using urine samples. This method is based on the observation that urine sediment consists of certain components derived from podocytes and/or tubular cells.

Why do patients with LBWN exhibit similar pathological changes to those observed in nephropathy patients with mtDNA mutations? It appears that the mitochondrial function of podocytes is involved in the formation of FSGS lesions, as we and others also recently proposed [17-21]. Although we cannot exactly evaluate the degree of foot process effacement by the limitation of sampling, mild foot process effacement were observed all our cases of LBWN. In the present study, we did not observe any increments in the number of mitochondria in the podocytes of the patients with LBWN, which is indeed a different pathology from that observed in mitochondrial cytopathy

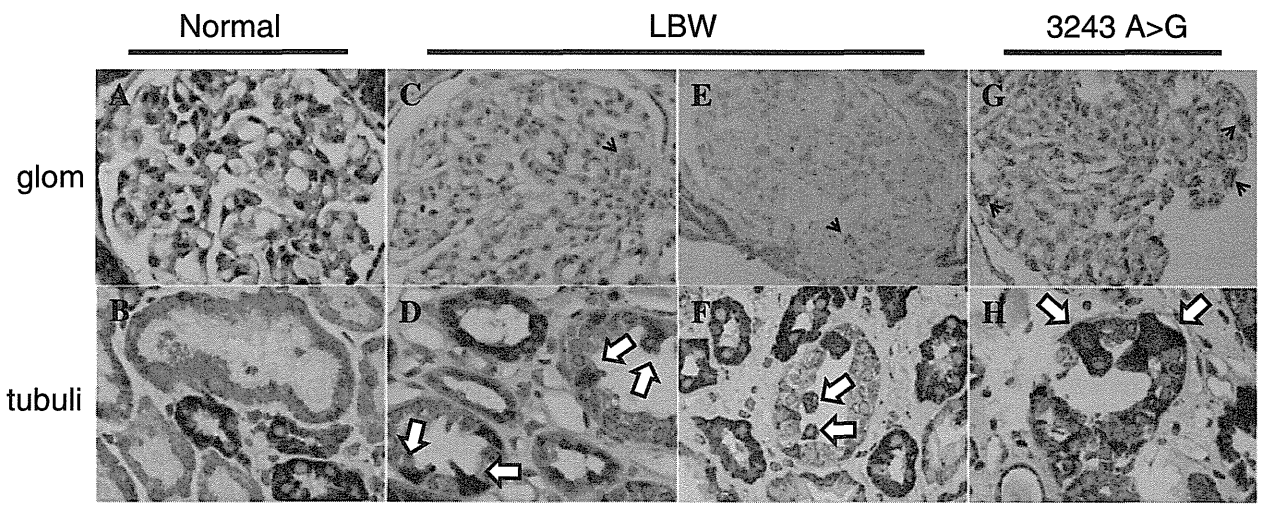

Figure 4 COX IV staining of the glomeruli and tubules. A: In the glomeruli of a normal control, the podocytes almost equally express COX IV. **B**. In the tubules of a normal control, the tubular cells at the same luminal level almost equally express COX IV. **C**. In the glomeruli of LBW 1, only one podocyte (arrow) expresses more COX IV than the other podocytes. **D**. In the tubules of LBW 1, unbalanced strong staining for COX IV is detected (arrows). Only a part of tubular cells express extremely intense COX IV compared with other tubular cells at the same luminal level. **E**: In the glomeruli of LBW 4, only one podocyte (arrow) expresses more COX IV than the other podocytes. **F**. In the tubules of LBW 4, staining for COX IV in a part of tubular lumens exhibits a mosaic pattern. The GSECs should express intense COX IV staining (arrows). **G**: In the glomeruli of Mt 1, a portion of podocytes (arrows) express more COX IV than the other podocytes. **H**: In the tubules of Mt 1, a portion of tubular cells are intensely stained (arrows) compared with the other cells in the same lumen. These cells should coincide with GSECs002E.

Table 2 Summary of the findings of nephropathy in the mitochondrial cytopathy and LBW-related nephropathy patients

	Normal	Mitochondrial cytopathy	LBW-related nephropathy
mtDNA mutation	No	Yes	No
FSGS lesion	No	Yes[1]	Yes
Glomerular hypertrophy	No	Yes or No	Yes
Foot process effacement	No	Yes	Yes
Increased mitochondria in podocyte	No	Yes	No
GSECs in tubules	No	Yes	Yes
COX IV expression in glomeruli	uniform	mosaic pattern	weak (but intense in a few podocytes)
COX IV expression in tubules	uniform	partially mosaic pattern	partially mosaic pattern

[1]Although the two patients with mitochondrial cytopathy had no FSGS lesions in the glomeruli, the presence of FSGS lesions is a characteristic glomerular change in mitochondrial cytopathy patients, as reported in many previous reports.

patients. However, an increased number of mitochondria is only one phenomenon underlying mitochondrial abnormalities and is easily detected pathologically. In fact, mitochondrial biogenesis is controlled by complex mechanisms [22]; therefore, we cannot deny the possibility of mitochondrial dysfunction in LBWN patients, even when an increased number of mitochondria is not observed. COX IV is one of the major components of complex IV, the last enzyme in the respiratory electron transport chain in mitochondria [23]. When we stained the kidney sections using anti-COX-IV antibodies, the staining intensity of podocytes and tubular cells ay the same luminal levels were uniform. However, in patients with mtDNA mutations, COX IV expression, which was mainly expressed by podocytes in glomeruli, showed mosaic patterns. Furthermore, a part of tubular cells with mtDNA mutations extremely expressed COX IV compared with other tubular cells at the same luminal levels (Figure 4). COX IV expression was not uniform in glomeruli of LBWN patients, too. A few podocytes expressed stronger COX IV compared with most of other podocytes. Only a part of tubular cells in LBWN patients expressed extremely intense COX IV as like those in patients with mtDNA mutations (Figure 4). Although we cannot judge whether an unbalanced COX IV expression directly affects the pathogenesis of kidney disease, our results suggest the possibility that the mitochondrial function, not mitochondrial DNA mutations, is associated with the etiopathogenesis of low birth weight-related nephropathy.

In addition, GSECs could be occasionally observed in aged patients. Therefore, GSECs might not be specific findings. However, because all of LBWN patients had GSECs in a part of their tubular cells, we think that GSECs in LBWN should be "meaningful" pathological changes. Furthermore, if GSECs are observed, especially in young patients, the analysis of mtDNA might be needed [24]. Now, we cannot explain why GSECs partially appear. Furthermore, it is obscure that a part of tubular cells show intense COX IV expression although most of tubular cells uniformly express COX IV at the same luminal levels. Although we now hypothesize that unbalance between high energy demand and low energy supply might result in mitochondrial dysfunction, further studies must be needed.

We cannot exclude the possibility that our four patients with LBWN had similar pathological lesions to those observed in the patients with mitochondrial cytopathy "by chance". In spite of these limitations, some specific cases with characteristic pathological findings should provide new aspects [25-27]. This report provides new clues regarding mitochondria to prompt investigations of the pathomechanisms underlying the renal dysfunction associated with LBW.

Conclusion

This is the first report to show the pathological similarities not only in glomeruli but also tubuli between nephropathy with a LBW history and nephropathy with mitochondrial cytopathy.

Abbreviations

LBW: Low-birth-weight; ESRD: End-stage renal disease; CKD: Chronic kidney disease; FSGS: Focal segmental glomerulosclerosis; LBWN: LBW-related nephropathy; COX IV: Cytochrome c oxidase subunit IV; GSECs: Granular swollen epithelial cells; MELAS: Mitochondrial myopathy, encephalopathy, lactic acidosis, stroke-like episodes.

Competing interests

All authors declared that they have no competing interest.

Authors' contributions

TI formed the study concept and organized this study. TM analyzed mtDNA mutations. NM, TK, RR and MN provided their efforts for making data and critical suggestions to this study. YY and HK analyzed renal pathology and provided expertise as renal pathologists. All authors read and approved the final manuscript.

Acknowledgements

All protocols described in this report followed the methods approved by the ethics committee. We thank Mori Tachibana for the technical assistance. This work was supported by the JSPS (Japan Society for the Promotion of Science) KAKENHI Grant Number 80348276 to T. Imasawa and a grant from the National Hospital Organization of Japan to T. Imasawa.

Author details
[1]Kidney Center, National Hospital Organization Chiba-East Hospital, 673 Nitona-cho, Chuoh-ku, Chiba-city, Chiba 260-8712, Japan. [2]Clinical Research Center, National Hospital Organization Chiba-East Hospital, Chiba-city, Chiba, Japan. [3]Department of Genomics for Longevity and Health, Tokyo Metropolitan Institute of Gerontology, Itabashi, Tokyo, Japan. [4]Aging Regulation Section, Tokyo Metropolitan Geriatric Hospital and Institute of Gerontology, Itabashi, Tokyo, Japan. [5]Yamaguchi Pathology Laboratory, Matsudo, Chiba, Japan. [6]EA4576 MRGM, University of Bordeaux, Bordeaux, Gironde, France.

Received: 2 May 2014 Accepted: 7 September 2014
Published online: 30 September 2014

References

1. Vikse BE, Irgens LM, Leivestad T, Hallan S, Iversen BM: **Low birth weight increases risk for end-stage renal disease.** *J Am Soc Nephrol* 2008, **19**:151–157.
2. Williams S, St George IM, Silva PA: **Intrauterine growth retardation and blood pressure at age seven and eighteen.** *J Clin Epidemiol* 1992, **45**:1257–1263.
3. Benediktsson R, Lindsay RS, Noble J, Seckl JR, Edwards CR: **Glucocorticoid exposure in utero: new model for adult hypertension.** *Lancet* 1993, **341**:339–341.
4. Hughson M, Farris AB 3rd, Douglas-Denton R, Hoy WE, Bertram JF: **Glomerular number and size in autopsy kidneys: the relationship to birth weight.** *Kidney Int* 2003, **63**:2113–2222.
5. Brenner BM, Meyer TW, Hostetter TH: **Dietary protein intake and the progressive nature of kidney disease: the role of hemodynamically mediated glomerular injury in the pathogenesis of progressive glomerular sclerosis in aging, renal ablation, and intrinsic renal disease.** *N Engl J Med* 1982, **307**:652–659.
6. Brenner BM, Lawler EV, Mackenzie HS: **The hyperfiltration theory: a paradigm shift in nephrology.** *Kidney Int* 1996, **49**:1774–1777.
7. Hodgin JB, Rasoulpour M, Markowitz GS, D'Agati VD: **Very low birth weight is a risk factor for secondary focal segmental glomerulosclerosis.** *Clin J Am Soc Nephrol* 2009, **4**:71–76.
8. Nishigaki Y, Ueno H, Coku J, Koga Y, Fujii T, Sahashi K, Nakano K, Yoneda M, Nonaka M, Tang L, Liou CW, Paquis-Flucklinger V, Harigaya Y, Ibi T, Goto Y, Hosoya H, DiMauro S, Hirano M, Tanaka M: **Extensive screening system using suspension array technology to detect mitochondrial DNA point mutations.** *Mitochondrion* 2010, **10**:300–308.
9. Doleris LM, Hill GS, Chedin P, Nochy D, Bellanne-Chantelot C, Hanslik T, Bedrossian J, Caillat-Zucman S, Cahen-Varsaux J, Bariety J: **Focal segmental glomerulosclerosis associated with mitochondrial cytopathy.** *Kidney Int* 2000, **58**:1851–1858.
10. Hotta O, Inoue CN, Miyabayashi S, Furuta T, Takeuchi A, Taguma Y: **Clinical and pathologic features of focal segmental glomerulosclerosis with mitochondrial tRNALeu(UUR) gene mutation.** *Kidney Int* 2001, **59**:1236–1243.
11. Guéry B, Choukroun G, Noël LH, Clavel P, Rötig A, Lebon S, Rustin P, Bellané-Chantelot C, Mougenot B, Grünfeld JP, Chauveau D: **The spectrum of systemic involvement in adults presenting with renal lesion and mitochondrial tRNA(Leu) gene mutation.** *J Am Soc Nephrol* 2003, **14**:2099–2108.
12. Matsuo S, Imai E, Horio M, Yasuda Y, Tomita K, Nitta K, Yamagata K, Tomino Y, Yokoyama H, Hishida A: **Revised equations for estimated GFR from serum creatinine in Japan.** *Am J Kidney Dis* 2009, **53**(6):982–992.
13. Kataoka H, Ohara M, Honda K, Mochizuki T, Nitta K: **Maximal glomerular diameter as a 10-year prognostic indicator for IgA nephropathy.** *Nephrol Dial Transplant* 2011, **26**(12):3937–3943.
14. Kobayashi A, Goto Y, Nagata M, Yamaguchi Y: **Granular swollen epithelial cells: a histologic and diagnostic marker for mitochondrial nephropathy.** *Am J Surg Pathol* 2010, **34**:262–270.
15. Stieger N, Worthmann K, Teng B, Engeli S, Das AM, Haller H, Schiffer M: **Impact of high glucose and transforming growth factor-β on bioenergetic profiles in podocytes.** *Metabolism* 2012, **61**:1073–1086.
16. Imasawa T, Fukuda N, Hirose S, Kato N, Shinya S, Yamamoto R, Kimura H, Kadomura M, Nishimura M, Yoshimura M, Ikei S: **Hemodialysis patients born with a low birth weight should have a different time course of kidney diseases than those born with a normal birth weight.** *Ther Apher Dial* 2013, **17**:293–297.
17. Diomedi-Camassei F, Di Giandomenico S, Santorelli FM, Caridi G, Piemonte F, Montini G, Ghiggeri GM, Murer L, Barisoni L, Pastore A, Muda AO, Valente ML, Bertini E, Emma F: **COQ2 nephropathy: a newly described inherited mitochondriopathy with primary renal involvement.** *J Am Soc Nephrol* 2007, **18**:2773–2780.
18. Heeringa SF, Chernin G, Chaki M, Zhou W, Sloan AJ, Ji Z, Xie LX, Salviati L, Hurd TW, Vega-Warner V, Killen PD, Raphael Y, Ashraf S, Ovunc B, Schoeb DS, McLaughlin HM, Airik R, Vlangos CN, Gbadegesin R, Hinkes B, Saisawat P, Trevisson E, Doimo M, Casarin A, Pertegato V, Giorgi G, Prokisch H, Rötig A, Nürnberg G, Becker C, *et al*: **COQ6 mutations in human patients produce nephrotic syndrome with sensorineural deafness.** *J Clin Invest* 2011, **121**(5):2013–2024.
19. Imasawa T, Rossignol R: **Podocyte energy metabolism and glomerular diseases.** *Int J Biochem Cell Biol* 2013, **45**(9):2109–2118.
20. Yamagata K, Muro K, Usui J, Hagiwara M, Kai H, Arakawa Y, Shimizu Y, Tomida C, Hirayama K, Kobayashi M, Koyama A: **Mitochondrial DNA mutations in focal segmental glomerulosclerosis lesions.** *J Am Soc Nephrol* 2002, **13**(7):1816–1823.
21. Hagiwara M, Yamagata K, Capaldi RA, Koyama A: **Mitochondrial dysfunction in focal segmental glomerulosclerosis of puromycin aminonucleoside nephrosis.** *Kidney Int* 2006, **69**(7):1146–1152.
22. Scarpulla RC: **Transcriptional paradigms in mammalian mitochondrial biogenesis and function.** *Physiol Rev* 2008, **88**(2):611–638.
23. Tsukihara T, Aoyama H, Yamashita E, Tomizaki T, Yamaguchi H, Shinzawa-Itoh K, Nakashima R, Yaono R, Yoshikawa S: **Structures of metal sites of oxidized bovine heart cytochrome c oxidase at 2.8 A.** *Science* 1995, **269**(5227):1069–1074.
24. Imasawa T, Tanaka M, Yamaguchi Y, Nakazato T, Kitamura H, Nishimura M: **7501 T > A mitochondrial DNA variant in a patient with glomerulosclerosis.** *Ren Fail* 2014, 1–5 [Epub ahead of print].
25. Zhang R, Zheng ZY, Lin JS, Qu LJ, Zheng F: **The continual presence of C3d but not IgG glomerular capillary deposition in stage I idiopathic membranous nephropathy in patients receiving corticosteroid treatment.** *Diagn Pathol* 2012, **7**:109.
26. Otani N, Akimoto T, Yumura W, Matsubara D, Iwazu Y, Numata A, Miki T, Takemoto F, Fukushima N, Muto S, Kusano E: **Is there a link between diabetic glomerular injury and crescent formation? A case report and literature review.** *Diagn Pathol* 2012, **7**:46.
27. Ferreira RD, Custódio FB, Guimarães CS, Corrêa RR, Reis MA: **Collagenofibrotic glomerulopathy: three case reports in Brazil.** *Diagn Pathol* 2009, **4**:33.

doi:10.1186/s13000-014-0181-0
Cite this article as: Imasawa *et al.*: Pathological similarities between low birth weight-related nephropathy and nephropathy associated with mitochondrial cytopathy. *Diagnostic Pathology* 2014 **9**:181.

RENAL FAILURE

http://informahealthcare.com/rnf
ISSN: 0886-022X (print), 1525-6049 (electronic)

Ren Fail, Early Online: 1–5
 DOI: 10.3109/0886022X.2014.945181

informa
healthcare

CASE REPORT

7501 T>A mitochondrial DNA variant in a patient with glomerulosclerosis

Toshiyuki Imasawa[1], Masashi Tanaka[2], Yutaka Yamaguchi[3], Takashi Nakazato[4], Hiroshi Kitamura[1], and Motonobu Nishimura[1]

[1]Kidney and Diabetes Center, National Hospital Organization Chiba-East Hospital, Chiba-city, Chiba, Japan, [2]Department of Genomics for Longevity and Health, Tokyo Metropolitan Institute of Gerontology, Itabashi, Tokyo, Japan, [3]Yamaguchi Pathology Laboratory, Matsudo, Chiba, Japan, and [4]Department of Cardiology, National Hospital Organization Chiba Medical Center, Chiba, Japan

Abstract

The presence of granular swollen epithelial cells (GSECs) in tubular cells was recently reported to be a specific change associated with mitochondrial cytopathy. However, at present, GSEC is not routinely evaluated. We, in this study, present a case of glomerulosclerosis, in which the presence of GSECs should provide us one clue to understand the pathogenesis of its progressive decline of renal function. A 54-year-old Japanese female, who had been diagnosed with Graves' disease, was referred for the examination and treatment of her proteinuria (5.4 g/gCre at the first visit to our hospital). A kidney biopsy showed 28.6% of the glomeruli to be globally sclerosed and 10.7% of the glomeruli to have completely collapsed. However, according to a light microscopic analysis, all other glomeruli showed an almost normal appearance, except for some slight enlargement. Almost 30% of the interstitium was damaged by fibrosis. Characteristically, GSECs were observed in the medulla collecting ducts. Although she had no symptoms of either myopathy or encephalopathy, no history of stroke-like episodes or difficulty in hearing, her serum concentrations of lactate and pyruvate were both elevated. Therefore, mitochondrial DNA sequencing was performed to assess the etiopathogenesis of her nephropathy. Consequently, a homoplasmic 7501 T>A replacement, which has not been previously reported in patients with renal diseases, was detected. This case suggests that the routine evaluation of GSECs can provide important clues to assess the etiopathogenesis of cryptogenic glomerulosclerosis.

Keywords

Glomerulosclerosis, granular swollen epithelial cell, mitochondria, mitochondrial DNA

History

Received 5 March 2014
Accepted 27 June 2014
Published online 1 August 2014

Introduction

The 3243 A>G mutation is one of the most frequently observed mutations of mitochondrial DNA (mtDNA). In the past two decades, many reports have described that the 3243 A to G mutation could cause focal segmental sclerosis (FSGS).[1–3] By electron microscopy, some podocytes were found to have an increased number of enlarged mitochondria in their cytoplasm. It was recently reported that patients with mitochondrial cytopathy have pathological changes not only in glomeruli but also in tubules. The characteristic pathological cells were designated as granular swollen epithelial cells (GSECs), because the cells include increased and enlarged mitochondria in their cytoplasm, which makes them look "swollen".[4]

We herein present a case of glomerulosclerosis accompanied with GSECs, in whom a new mtDNA variant, which has not been previously reported in patients with renal diseases, was detected.

Address correspondence to Toshiyuki Imasawa, MD, PhD, Kidney and Diabetes Center, National Hospital Organization Chiba-East Hospital, 673 Nitona-cho, Chuoh-ku, Chiba 260-8712, Japan. Tel: +81 43 261 5171; Fax: +81 43 268 2613; E-mail: imasawa@cehpnet.com

Case

This case was a 54-year-old Japanese female, who was referred to Chiba-East Hospital by her primary doctor in order to examine and treat her proteinuria. When she was 50 years old, cardiomegaly had been pointed out by the chest X-ray taken during an annual health check-up, although she had no symptoms. She visited her primary doctor and was diagnosed to have Basedow's disease (thyroid-stimulating hormone; TSH<0.002 μIU/mL, FT3 6.0 pg/mL, FT4 2.4 ng/mL, TSH receptor antibody 50.5%) and atrial fibrillation (Af). Therefore, she had been prescribed propylthiouracil (PTU) and digoxin. At 52 years of age, her blood glucose level was elevated, and she was diagnosed with diabetes mellitus (DM). Thereafter, she had also been taking a dipeptidyl peptidase 4 inhibitor. Beginning when she was 53 years old, the patient's urinary examination by the test tape started to show proteinuria from 1+ to 3+. She had also been prescribed an angiotensin II receptor blocker to treat hypertension for three months until the first visit to Chiba-East Hospital. At the first

visit, her blood pressure was 157/117 and the proteinuria was 5.4 g/gCre, although the serum albumin level was 4 mg/dL. She had moderate pretibial pitting edema (PTPE).

Because she reported consuming a lot of salt, she was recommended to start a low salt diet (under 6 g/day of salt). One month after the first visit to our hospital, she was admitted in order to undergo examinations due to proteinuria. At this admission, her blood pressure was 139/93 without any change in the drugs being administered at the first visit, and her PTPE had disappeared. The proteinuria also had decreased to 1.5 g/gCre. A physical examination showed a height of 153.1 cm, body weight of 54.1 kg and body mass index of 23.1. No crackles or murmurs were detected on chest auscultation. Although she had been suffering from DM for two years, no evidence of diabetic neuropathy was observed. No skin lesions were detected. An ophthalmologic examination detected neither diabetic retinopathy nor hypertensive retinopathy. Thyroid enlargement was also not detected by palpation.

The patient's birth weight had been 3500 g at 40 weeks of gestation. Her mother suffered from DM, and her father suffered from a kidney disease whose etiology had not been assessed. She was not a smoker. Laboratory tests on admission (Table 1) showed slightly elevated serum creatinine and positive myeloperoxidase-anti-neutrophil cytoplasmic antibody (MPO-ANCA). However, no signs of vasculitis were detected. We concluded that PTU likely triggered this MPO elevation.[5]

Electrocardiography showed Af (heart rate: 51 bpm) and moderate down-sloping ST depression and inverted T waves on leads I, II, aVF, V4-6, which could be explained by the digitalis effect. On chest X-rays, although severe cardiomegaly (cardiothoracic ratio, 67.1%) was detected, there was neither enlargement of the pulmonary artery shadow nor pleural effusion. An echogram of the thyroid revealed no swelling on either side and no masses. We performed a percutaneous renal biopsy under ultrasound guidance two days after admission to investigate the etiology of the heavy proteinuria.

The light microscopic photos of the kidney biopsy specimen are shown in Figure 1. We obtained 28 glomeruli. There were eight glomeruli (28.6%) with global sclerosis and three glomeruli (10.7%) whose tufts were completely collapsed. However, all other glomeruli showed an almost normal appearance without any sclerotic lesions, tuft adhesions, endocapillary proliferation or crescent formations. Slight enlargement of all glomeruli was detected. Almost 30% of the area of the interstitium was damaged with fibrosis, but there were no inflammatory cells. Interestingly, GSECs were observed in the medulla collecting ducts (Figure 1). The arteriole endothelium showed slight hyalinosis, and the vascular smooth muscle cells of the arterioles were enlarged. Endothelial hyalinosis was previously reported as a pathological finding of mitochondria cytopathy. An electron microscopic analysis (Figure 2) showed moderate foot process effacement and moderate thickening of glomerular basement membrane. In all podocytes observed, there were no increases in the numbers of mitochondria in the cytoplasm. However, we found an increase number of enlarged mitochondria in the tubular cells.

As GSEC was previously reported to be a specific change associated with mitochondrial cytopathy, we measured serum lactate and pyruvate concentrations. These serum concentrations were elevated at 22.9 mg/dL (normal: 3.0–17.0) and 2.10 mg/dL (normal: 0.30–0.94), respectively. Therefore, we suspected a mtDNA mutation and examined the patient's

Table 1. The findings of laboratory tests performed on admission.

Blood cell count		Blood chemistry		Immunology		Hormones	
WBC	8000/mL	TP	8.1 g/dL	ASO	56 U/mL	TSH	1.45 μIU/ml
RBC	5.10×10^6/mL	Alb	4.3 g/dL	C3	133 mg/dL	fT3	2.97 pg/ml
Hb	14.9 g/dL	AST	24 IU/L	C4	22.3 mg/dL	fT4	1.45 ng/dl
Hct	45.2%	ALT	18 IU/L	IgG	1891 mg/dL		
MCV	89 fl	LDH	225 IU/L	IgA	183 mg/dL	Urinalysis	
MCHC	33.0%	ALP	150 IU/L	IgM	248 mg/dL	Gravity	1.010
Platelet	25.1×10^4/mL	Tbil	0.9 mg/dL	RA test	(–)	pH	5.5
		BUN	15.6 mg/dL	ANA	(–)	RBC	0–1 /HPF
Coagulation		Cr	0.76 mg/dL	M protein	(–)	WBC	0–1 /HPF
APTT	34.0 sec	UA	9.4 mg/dL	HBs antigen	(–)	Ccr (24 hr)	63.3 mL/min
PT(%)	86%	Tcho	214 mg/dL	HCV antibody	(–)	Protein	0.68 g/day
INR	1.1 INR	CRP	0.22 mg/dL	MPO-ANCA	67.5 EU	NAG	4.3 U/L
		FBS	126 mg/dL	PR3-ANCA	<10 EU	β2-MG	<20 mg/L
		HbA1c	7.5%	TSHrAb	3.8 IU/l	BJP	(–)
		digoxin	1.4 ng/ml				

Aberrant values are underlined.

WBC, white blood cells; RBC, red blood cells; Hb, hemoglobin; Hct, hematocrit; MCV, mean corpuscular volume; MCHC, mean corpuscular hemoglobin; APTT, activated partial thromboplastin time; PT, prothrombin time; INR, international normalized ratio; TP, total protein; Alb, albumin; AST, aspartate aminotransferase; ALT, alanine aminotransferase; LDH, lactate dehydrogenase; ALP, alkaline phosphatase; Tbil, total bilirubin; BUN, blood urea nitrogen; Cr, creatinine; UA, uric acid; Tcho, total cholesterol; CRP, C-reactive protein; FBS, fasting blood sugar; HbA1c, hemoglobin A1c (NGSP); ASO, antistreptolysin-O; C3, complement 3; IgG, immunoglobulin G; RA, rheumatoid arthritis; ANA, antinuclear antibody; M protein, monoclonal protein; HBs, hepatitis B surface; HCV, hepatitis C virus; MPO-ANCA, myeloperoxidase-anti-neutrophil cytoplasmic antibody; PR3, proteinase 3; TSHrAb, thyroid-stimulating hormone receptor antibodies; fT3, free triiodothyronine; fT4, free thyroxin; Ccr, creatinine clearance; NAG, N-acetylglutamate; MG, microglobulin; BJP, Bence Jones protein. To convert Hb, TP and Alb in g/dL to g/L, multiply by 10; Tbil in mg/dL to μmol/L, multiply by 17.1; BUN in mg/dL to mmol/L, multiply by 0.357; Cr in mg/dL to μmol/L, multiply by 88.4; UA in mg/dL to μmol/L, multiply by 59.48; Tcho in mg/dL to mmol/L, multiply by 0.02586; C3, C4, IgG, IgA and IgM in mg/dL to g/L, multiply by 0.01; and Ccr in mL/min to mL/sec, multiply by 0.01667.